Article | Received 3 December 2024; Accepted 7 February 2025; Published 20 February 2025
https://doi.org/10.55092/sc20250003

Monitoring of ground and building settlements induced by tunneling based on terrestrial LiDAR data: a case study in Singapore

Xinchen Zhang[1], Jiajun Li[2], Siau Chen Chian[3] and Qian Wang[4,*]

[1] College of Civil Engineering, Nanjing Tech University, Nanjing 211816, China
[2] Institute for Infrastructure and Environment, School of Engineering, The University of Edinburgh, Edinburgh EH9 3FB, UK
[3] Department of Civil and Environmental Engineering, National University of Singapore, Singapore 117576, Singapore
[4] Department of Construction and Real Estate, School of Civil Engineering, Southeast University, Nanjing 211189, China

* Correspondence author; E-mail: qianwang@seu.edu.cn.

Highlights:

- LiDAR-based method monitors ground and building settlements with millimeter accuracy.
- Local scan-based method outperforms full area registration in settlement measurement.
- Proposed method reduces manual effort, enhancing efficiency in tunneling-induced settlement monitoring.

Abstract: Ground and building settlements induced by tunneling excavation are common in cities. Such settlements can cause instability of the ground and threaten the safety of the upper infrastructures or buildings. Hence, it is vital to monitor the settlements during tunnel excavation to identify any potential risk. The current approach for settlement monitoring relies on manual measurements, which suffers from low efficiency and high labor cost. To improve monitoring efficiency, this study presents a settlement monitoring method based on terrestrial LiDAR data, which mainly consists of rough and fine alignment steps. Algorithms are developed to automatically process the 3D point cloud data obtained from terrestrial LiDAR and obtain settlement values for grounds and buildings. The proposed technique was applied and validated in a region with on-going tunneling works in Singapore. Different monitoring strategies including local-scan based method and registration-based method were examined and compared in this case study. Results demonstrated that the local scan-based monitoring method could yield more accurate settlement measurements compared with the traditional survey method. Registration-based method had higher calculation efficiency but with insufficient accuracy. In general, it is demonstrated that the LiDAR based settlement monitoring method is feasible in engineering

practice, with measurement errors controlled within 2–3 mm, and has great potential to improve efficiency and reduce labor cost required by the traditional method.

Keywords: settlement monitoring; terrestrial LiDAR; 3D point cloud; structural health monitoring

1. Introduction

Traffic congestion in big cities is becoming significant nowadays and leads to the development of underground transportation spaces, such as tunnels. Tunnel excavation will strongly affect the safety of existed subsurface structures or pedestrian and vehicle traffic [1–4]. In recent years, monitoring of ground settlement with novel sensing techniques has attracted great attentions in engineering communities. Compared with traditional settlement measurement methods based on total stations, novel sensing techniques can help to reduce the labor force required with an acceptable accuracy. For example, Klar *et al.* [5] presented an investigation on ground displacement monitoring based on distributed fiber optic sensing. The technique was evaluated in field investigations including a 3 m diameter tunnel at a depth of 18 m and a reliable ground displacement model was developed. More straight forward methods based on 'images' rather than sensor deployment, such as SAR interferometry and photogrammetry, were adopted by researchers to monitor the tunneling induced ground movements [6,7]. SAR interferometry is a powerful tool that can capture the surface deformation with centimeter accuracy. Roccheggiani *et al.* [7] conducted an MT-InSAR analysis to find out the evolution of tunneling caused ground displacements based on the data acquired from satellite. Results showed the reliability of the technique on monitoring of ongoing infrastructures. Zhang *et al.* [6] presented a method to identify the temporarily coherent points (TCP) between two SAR acquisitions and proposed a TCP registration method to further measure the ground settlement of Hong Kong Airport area. Over the past decades, the rapid progress in camera technology has enabled photogrammetry to be exploited extensively for civil engineering for its low cost, high quality and ease-of-use. The technology has been applied in volume calculation for geomorphology purpose [8,9], infrastructure condition assessment [10] and landslip [11]. Koch *et al.* [12] presented a review of detecting the defect and assessing the condition of bridge, tunnels, pipes and asphalt pavement. It is summarized that the current state-of-the-art computer vision based methods successfully support the automation of detecting and localizing defects. Chen *et al.* [11] studied a typical landslide triggered by Wenchuan Earthquake of 12 May 2008 based on a proposed model with remote sensing and digital terrain model data. Results indicate a good accuracy and reliability of the proposed model for calculation of the landslip volume.

Although the above methods show good engineering application potentials, there still exist some limitations on the application scenarios. For example, if the settled ground is blocked by objects, such as viaduct in cities, the images taken at high places by satellite cannot capture the settlement of the ground. Moreover, the accuracy of photogrammetry is often in centimeter level, which cannot satisfy the millimeter-level accuracy requirement in settlement monitoring. The data processing for photogrammetry is also time-consuming, which limits the acquisition of settlement measurements in a timely manner. Therefore, a more automated and accurate measurement technique based on remote sensing data at ground is required to monitor the settlement in cities.

The Light Detection And Ranging (LiDAR), also known as 3D laser scanning, is an emerging 3D sensing technology to acquire the geometric information of object surfaces. A LiDAR can measure the

distance to a target by emitting laser beams and detecting the reflected signals from the target. As a result, a dense and accurate 3D point cloud (PC) dataset containing all the distance measurements will be generated. LiDAR can be classified into two categories based on working platforms, namely ground LiDAR, and mobile LiDAR. A ground LiDAR, also known as terrestrial laser scanner, is usually mounted on a tripod positioned over the ground while it is under operation. The ground LiDAR has the highest ranging accuracy and therefore, has been utilized for applications that require high accuracy such as surveying [13–16], documentation [17–20], and monitoring of buildings and civil infrastructures [21–25]. Oskouie *et al.* [22] monitored the displacement of highway retaining walls during construction based on a LiDAR system. Results indicate that small-scale changes on the wall's displacement can be identified by extracting and comparing geometric features from 3D point clouds. Su *et al.* [17] scanned an excavation site of a six-story building with two underground story by a laser scanner on Northwestern University campus. The terrain geometry in three dimensions was acquired and the information could be used for correlating measured ground deformations. Kurdi *et al.* [26] modelled building façade and road based on point cloud and proved the efficiency in survey work. Meanwhile, with the development of machine learning technology, the processing of topography and surface feature identification of point cloud data have also become automated [27] Based on the applications of LiDAR stated in available literatures, using LiDAR for monitoring ground settlements induced by tunnel excavation is therefore expected to be feasible.

In this paper, a methodology to utilize LiDAR data for analyzing the ground settlement induced by tunnelling in an effective way is proposed. The methodology is adopted for measuring the ground settlement of a major road in Singapore. The settlement measurements from the proposed method are compared to the measurements from the traditional survey method, which is considered as the ground truth value. Two monitoring strategies including local scan-based method and full area registration-based method are also compared in the case study. The rest of this paper is organized as follows. Section 2 introduces the site of the case study and its characteristics. Section 3 illustrates the proposed methodology for settlement monitoring including data acquisition and data processing. Then, the experimental results are presented and discussed in Section 4. Finally, Section 5 summarizes this study and suggests future work. This paper makes a contribution to the application of point cloud technology for the monitoring of road and building settlement. It mainly lies in proposing and comparing various settlement monitoring schemes, verifying the monitoring accuracy of different schemes, and providing a reference for subsequent related research and applications.

2. Description of studied area

The monitored area was along a major road located in the southern part of Singapore, as shown in Figure 1. This road was initially developed through the reclamation of mangrove swamps and mudflats. Due to the development of rail-based urban transport system (also known as, Mass Rapid Transit, MRT), a section of the subway was planned to be constructed by means of tunnel boring beneath the major road.

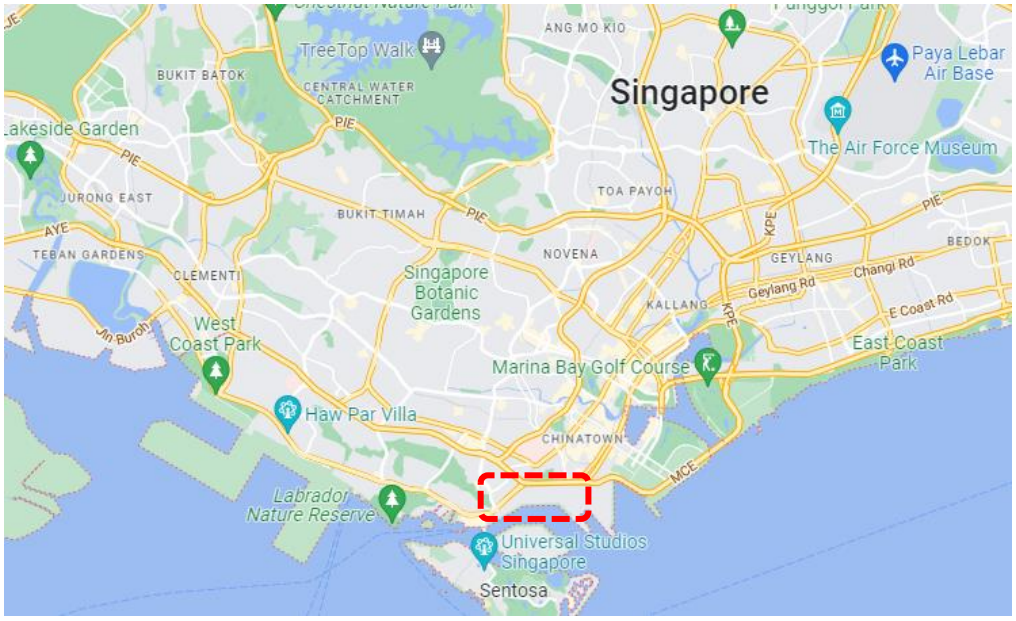

Figure 1. The monitored road with tunnel boring in Singapore (From Google Map).

In this study, the monitored areas are all located between two upcoming MRT stations. The existing ground level in the area is in the range of 15 m to 25 m above the rail level according to the tunneling report. Three specific locations in the region named as A1, A2 and A3 are selected for settlement monitoring, as roughly indicated in Figure 2.

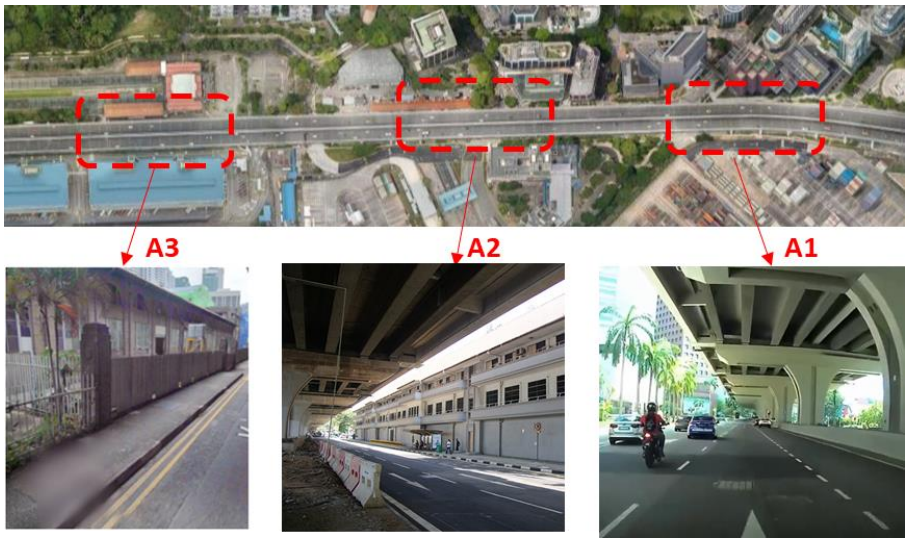

Figure 2. Three specific monitored locations (A1, A2, and A3).

A1 is the east part of the monitoring region along the 3-lane carriageway. Sparse trees and some high-rise buildings can be found on the north side of the road. In terms of the south side, only few trees can be observed. Road junction crossing is located within this area. The environment of A2 is slightly different from A1. At the north side, low-rise buildings could be found without trees. However, trees are very dense at the south side. A road crossing is also located at this region. For both A1 and A2, the road ground settlement is the target for monitoring. At A3, the tunneling path is beneath an existing monument building. Therefore, the settlement of the building will be monitored as well.

3. Proposed settlement monitoring method

The proposed settlement monitoring method has four steps. Firstly, the point cloud data are acquired by a LiDAR at specific areas on different dates, as explained in Section 3.1. Secondly, the acquired raw scans are registered before settlement calculation, as illustrated in Section 3.2. Thirdly, to calculate the settlement of a certain area over a period, the two point cloud datasets acquired on different dates should be aligned based on the settlement-free region. The alignment process includes two steps: rough alignment and fine alignment, as illustrated in Section 3.3 and 3.4, respectively. Lastly, the settlement of a certain area over a period is calculated by comparing the elevation values of two point cloud datasets at the settlement region, which will be explained in Section 3.5. A flowchart for explaining the proposed method is illustrated in Figure 3.

Figure 3. Flowchart for the proposed method.

3.1. Data acquisition

To enable the measurement of settlements, the obtained point cloud data must cover both settlement region and settlement-free region. The settlement region refers to the region that is relatively close to the tunnelling path and therefore can have certain settlements. The settlement-free region refers to the region that is sufficiently far away from the tunnelling path and therefore is unlikely to have settlements. In this case study, at A1 and A2, one side of the road belongs to the settlement region and the other side of the road belongs to the settlement-free region. Hence, both sides of the road should be scanned. At A3, the monument building belongs to the settlement region while the external roads next to the building are located outside of the influence zone (*i.e.* settlement-free region).

Due to the large size of each area (A1 to A3), multiple scans are needed to cover each area. For example, a total of ten scans at various locations were conducted at A1 for each time of monitoring. The exact locations and the registered point could data for A1 are illustrated in Figure 4. In terms of A2, a total of 13 scans were conducted for each time of monitoring. The corresponding positions and the registered point cloud data are shown in Figure 5. The average overlapping ratio between adjacent scans at A1 and A2 was around 66%. At A3, a total of eight scans at various positions around the monument building façade were conducted.

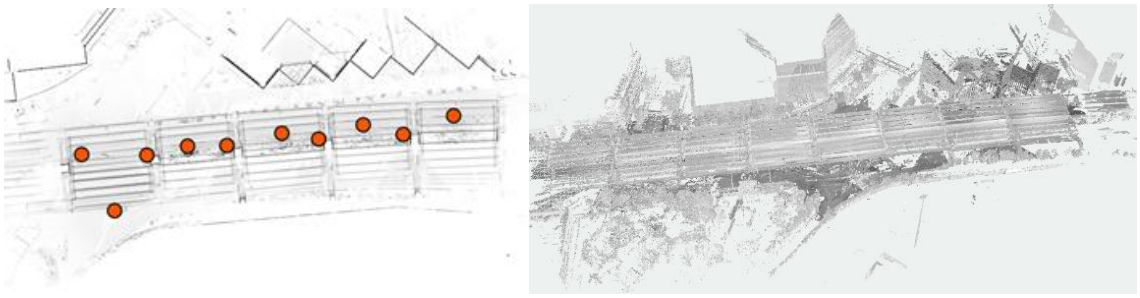

Figure 4. Scan locations and registered point cloud data of A1.

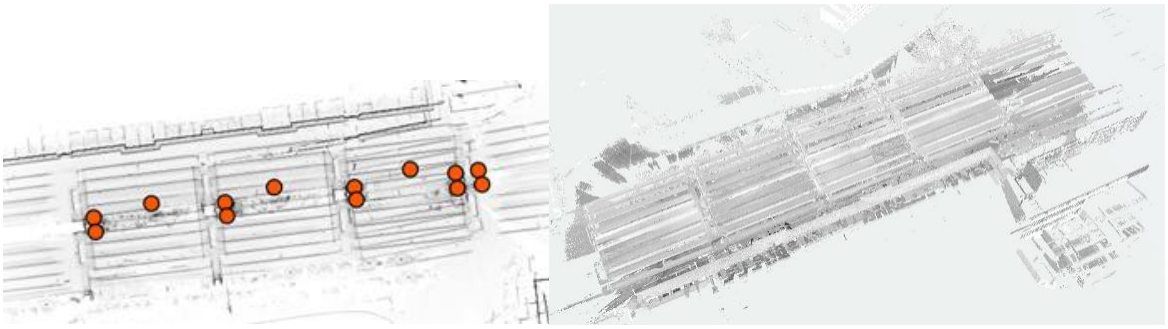

Figure 5. Scan locations and registered point cloud data of A2.

In this study, the 3D point cloud data were collected by a FARO S70 terrestrial LiDAR under clear sky conditions. The scanning resolution and quality was set as 1/4 and 2x in the scanner setup, corresponding to an angular resolution of 0.036° for all scanning locations. Each of the three areas was scanned on four or five different dates with an interval of four days for monitoring the settlement induced by the ongoing tunneling process.

3.2. Data registration

The obtained raw scans must be registered before the calculation of settlement values. There are two different strategies for data registration and settlement calculation. The first strategy is known as full area registration-based method. This strategy is to register all scans in a certain area, such as all ten scans at A1, and obtain a registered scan dataset for the entire area. Then, the point cloud datasets of the entire area on two different dates will be compared for settlement calculation. The advantage of this strategy is that only one comparison is needed to find out the settlement vlaues on the entire area over a period. However, this strategy can suffere from large registration errors. It is worth mentioning that the registration of point cloud data from two sites will generate a certain amount of error, and as the number of registered sites increases, this error may be magnified. Although this error is relatively small in terms of the scale of the entire scanning scene, it may cause significant interference with the accuracy of settlement monitoring values.

The second strategy is known as local scan-based method. This strategy will not register all scans in an entire area. Instead, this strategy uses only point cloud data of a local area for settlement calculation. In this case study, this strategy will use only one or two scans at a local area for settlement measurement. The advantage of this strategy is that there is minimum registration error among scans. Meanwhile, as the entire area is divided into several local areas, a few comparisons are needed to obtain the settlement values of the entire area over a period.

In this case study, it is found that the first strategy suffers from serious registration errors, and cannot provide accurate settlement measurements. Therefore, the local scan-based method is adopted finally. The local scan-based method comes in two forms: single scan and two-scans registration. When a single scan can capture both the settlement region and settlement-free region, the settlement values will be measured based on only the single scan. However, in some scenarios, one single scan cannot capture both regions. For example, due to the existence of viaduct piers, one single scan at A2 can only capture one region (*i.e.* one side of the road), and cannot fully capture the other region (*i.e.* the other side of the road), as shown in Figure 6(a). In this case, two scans are conducted and registered to capture both the

settlement region and settlement-free region at the local area, as shown in Figure 6(b). In the case study, the single scan method is mostly used in A1 and A3 due to few occlusions. For A2, the two-scans registration method is adopted due to more serious occlusions.

(a) Single scan. (b) Two-scans registration.

Figure 6 An example of single scan and two-scans registration method.

3.3. Rough alignment

The step of rough alignment aims to roughly align two point cloud datasets on different dates. The rough alignment is conducted in the FARO SCENE software in the following two steps. The first step is to find the same plane on the viaduct pier or other objects in different point cloud datasets to align the two datasets to the same direction, as shown in Figure 7.

Figure 7. Step 1—Align the direction based on a plane.

After the direction alignment, the origin coordinate in different datasets should be set as the same. As shown in Figure 8, the same point on the settlement-free region is found from two datasets and is set as the origin coordinate. It should be noted that sometimes it is not easy to select the same point from two different datasets. Therefore, the point on an object corner or at a place with distinctive features is suggested to be selected.

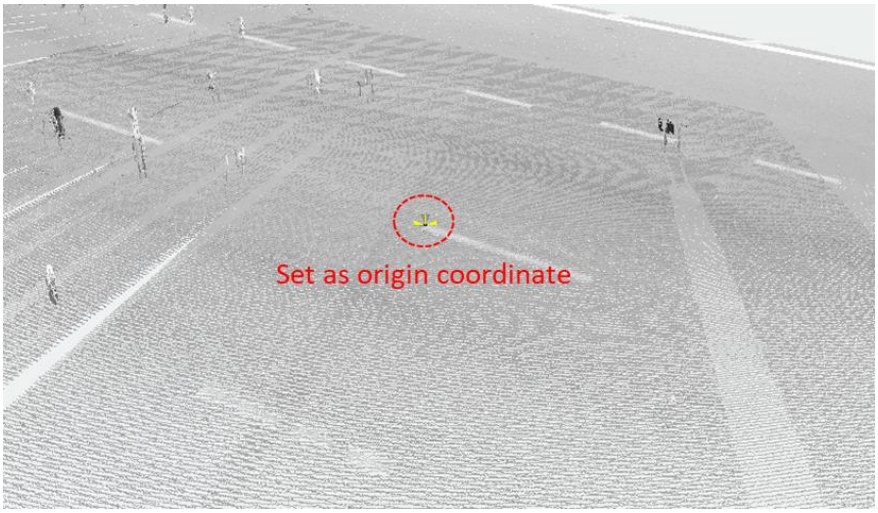

Figure 8. Step 2—Align the origin coordinate based on a point in settlement-free region.

After the above rough alignment procedures in SCENE software, the data will be exported as XYZ coordinates for further fine alignment in MATLAB.

3.4. Fine alignment

The step of fine alignment is required because the point cloud datasets can still have mis-alignment after the rough alignment step. The fine alignment between two point cloud datasets is conducted in MATLAB as follows. The first step is to pick out an identical area in settlement-free region with good data quality from different point cloud datasets. In this case study, the road surface or ground surface are selected.

After that, the Z coordinates of points in this area from different point cloud datasets are compared, as illustrated in Figure 9. Then, the ΔZ values between two datasets are obtained, and a plane is fitted to the ΔZ values, as shown in the right-hand figure in Figure 9. Finally, one point cloud dataset will be transformed such that the fitted plane of the ΔZ values become horizontal and equal to zero. This is to ensure that the settlement-free regions of the two point cloud datasets are perfectly aligned, which is essential for the following calculation of settlement values in the settlement region.

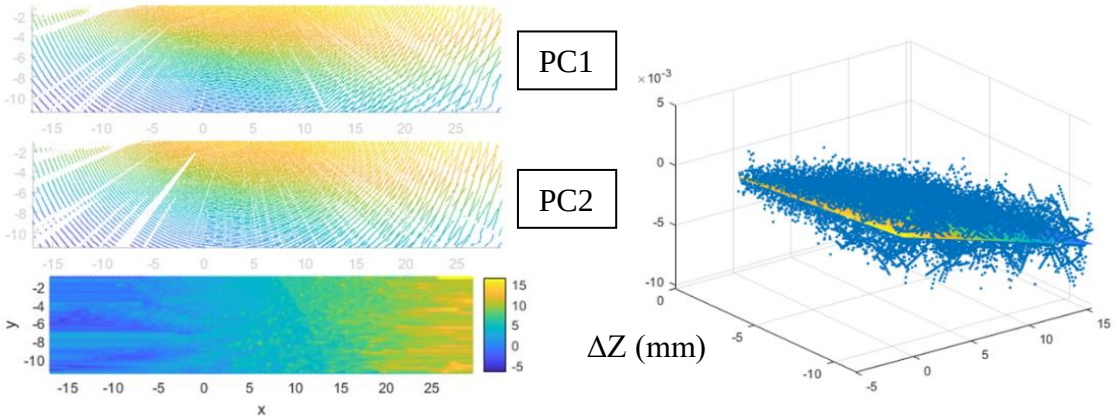

Figure 9. Fine alignment between two point cloud datasets based on the fitted plane of ΔZ values.

3.5. Settlement calculation

After fine alignment, the two point cloud datasets are well aligned based on the settlement-free region. Therefore, the ΔZ values between two datasets at the settlement region can be calculated and become the settlement measurements.

Figure 10 shows an example of point cloud datasets after fine alignment for settlement calculation. The top figure shows a cross section of two point cloud datasets, which are shown in red and blue colors. The left part is the settlement-free region while the right part is the settlement region. After fine alignment, it can be observed that the red and blue lines are perfectly aligned for the settlement-free region, such as the marked region 1 in Figure 10. On the other hand, the red and blue lines show clear differences for the settlement region, such as the marked region 2 in Figure 10, which indicate settlement changes between two dates.

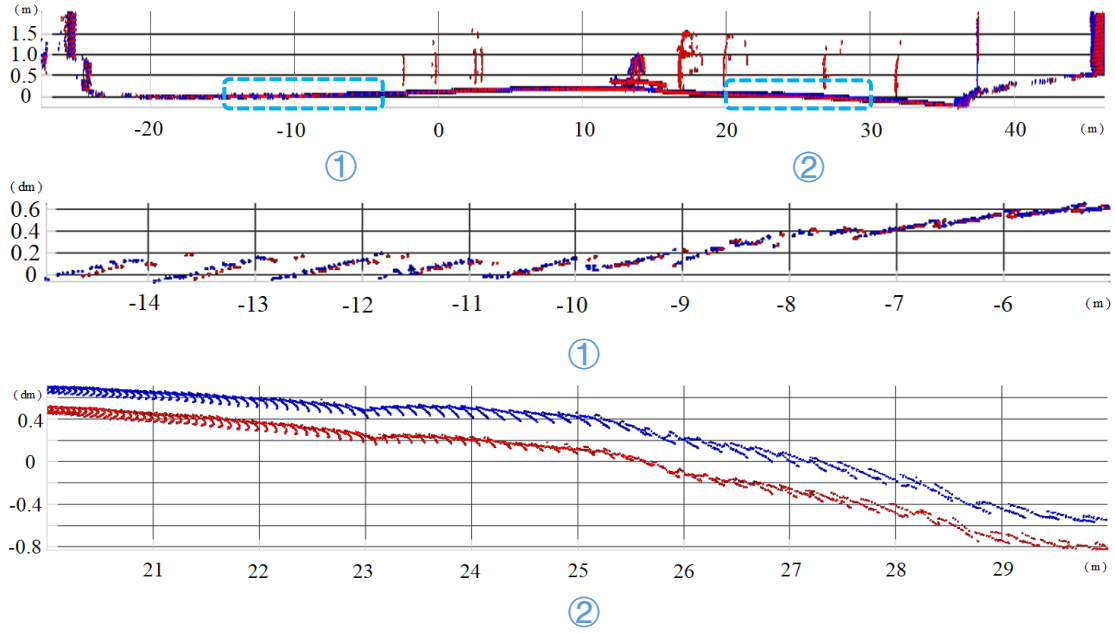

Figure 10. Example of point cloud datasets after fine alignment for settlement calculation.

4. Results and discussions

In the case study, there are a series of ground settlement markers or building settlement markers placed at the settlement region of A1, A2 and A3. The settlement values of the markers obtained through LiDAR data are compared with the traditional monitoring method, *i.e.*, survey by total stations. Therefore, the accuracy of the LiDAR-based method can be obtained by assuming that the traditional survey results are the ground truth values. The detailed results and comparison at different monitoring regions are demonstrated in the following sections.

4.1. Results at A1

At A1, the single scan method is adopted for settlement monitoring. The selected settlement markers in this region are shown in Figure 11. These markers are located at a road crossing and can be captured by the scanner placed at the viaduct pier at two sides of the crossing. Table 1 lists the monitored settlement

values at the above-mentioned markers. The values outside the brackets are the settlement values obtained from LiDAR data while the values in the brackets are the measurements from the traditional survey method. The point cloud data are acquired on five different days, where day 1 is considered as the baseline and the settlement values of the other days are calculated by comparison with day 1.

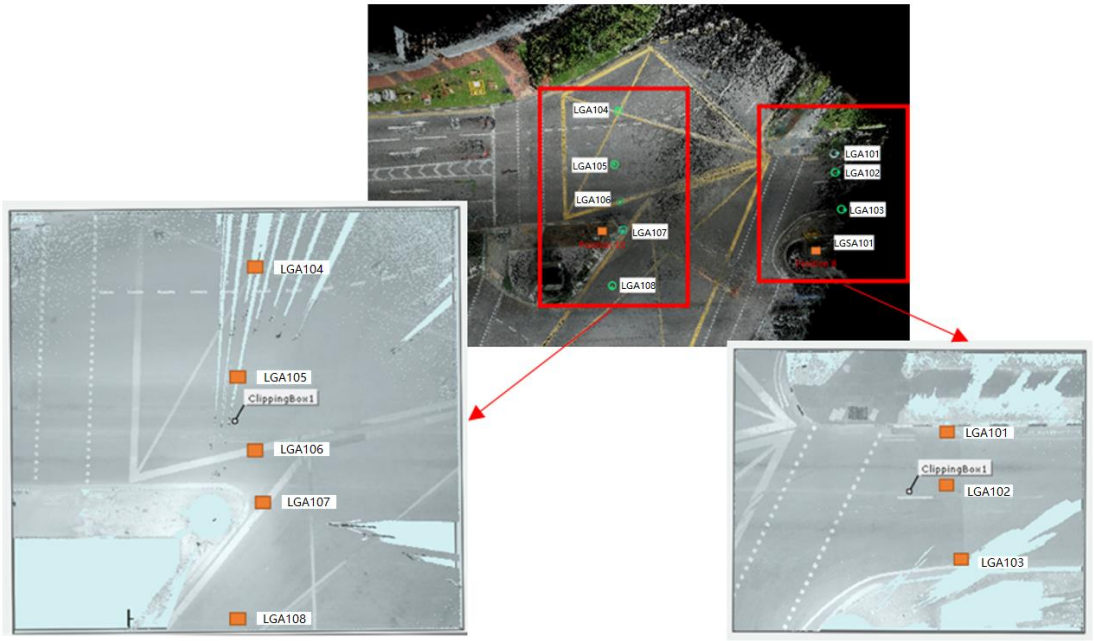

Figure 11. Ground settlement markers at A1.

Table 1. Settlement values at A1.

Marker	LG A101	LG A102	LG A103	LG A104	LG A105	LG A106	LG A107	LG A108
Day 1				Baseline				
Day 2	NA (1.7)	NA (-4.2)	NA (-0.2)	-0.1 (0.0)	-1.3 (-7.1)	-1.7 (-6.5)	-1.1 (-0.4)	0.1 (0.8)
Day 3	6.6 (1.1)	8.4 (-3.7)	2.0 (0.2)	2.4 (-1.8)	2.9 (-6.8)	1.9 (-6.2)	2.6 (0.3)	-0.8 (1.1)
Day 4	29.5 (31.7)	18.4 (17.9)	7.2 (7.2)	20.4 (5.9)	21.1 (-3.2)	10.6 (-3.0)	1.5 (5.0)	-1.0 (4.3)
Day 5	27.4 (25.3)	25.6 (19.6)	14.3 (8.1)	-3.2 (12.4)	-1.8 (15.9)	0.4 (6.0)	-0.9 (7.3)	-0.5 (3.8)

It could be noticed that in certain days, the results calculated based on point clouds are quite close to the measured results based on traditional survey. For example, on day 4 and day 5, the results of marker LGA101, LGA102 and LGA103 are quite close. However, the results of LGA104 to LGA105 are not that good on the same day compared with previous ones. Assuming that the values from traditional survey are the ground truth, the mean error and standard deviation of measurements from LiDAR data are 6.5 mm and 5.9 mm, respectively. These results indicate that the single scan method has limited accuracy. By checking the obtained LiDAR data, it is found that the point cloud data cannot fully capture the settlement-free region due to occlusions, which may affect the accuracy of rough and

fine alignments and the following settlement calculation. Based on lessons learnt from A1, the two-scans registration method is adopted at A2, which has more serious occlusions.

4.2. Results at A2

At A2, the two-scans registration method is adopted for settlement monitoring. For each local area, two scans located on the two sides of the viaduct pier are conducted, as indicated in Figure 6(b). The positions of selected settlement markers are illustrated in Figure 12. Table 2 lists the settlement values from LiDAR data and traditional survey at the settlement markers.

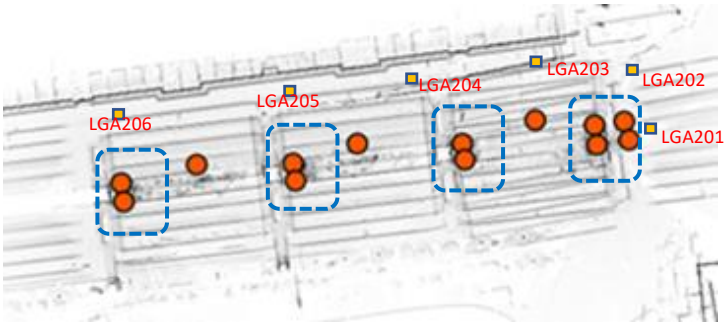

Figure 12. Selected settlement markers at A2.

Table 2. Settlement values at A2.

Marker	LGA201	LGA202	LGA203	LGA204	LGA205	LGA206
Day 1			Baseline			NA
Day 2	0.3 (-0.4)	1.4 (-0.3)	0.5 (-0.5)	-3.2 (0.4)	0.5 (2.7)	Baseline
Day 3	NA	NA	NA	-0.2 (0.3)	-2.1 (-1.1)	1.1 (-3.5)
Day 4	NA	NA	NA	NA	3.6 (0.9)	2.9 (-1.3)

It can be observed from Table 2 that the error of LiDAR-based measurements compared to traditional survey results is significant reduced. The error is ranging from 0.5 mm to 4.6 mm and the average error is only 2.2 mm with a standard deviation of 1.4 mm. Owing to the intact information of the settlement-free region due to two-scans registration, the accuracy of the rough and fine alignments is significantly improved compared to the single scan method at A1.

4.3. Results at A3

At A3, the monitored object is the monument building and the ground around it. The single scan method and two-scans registration method are both used at A3. If the settlement-free region cannot be covered by a single scan, the two-scans registration method is then adopted. The building settlement markers (BM series) and ground settlement markers (LG series) at A3 are demonstrated in Figure 13.

Figure 13. Positions of building and ground settlement markers at A3 (From Google Map).

The calculation of ground settlement at A3 is similar to A1 and A2. However, the calculation of building settlement is different. Although building settlement markers are often installed on building façade, it is impossible to calculate building settlement based on the point cloud data of vertical building façade. Instead, it is much easier to calculate the building settlement based on horizontal elements in the building. Therefore, locations such as the horizontal surfaces at building arch and window openings are selected near certain settlement markers for building settlement calculation, as shown in Figure 14.

Most of the settlement markers at A3 are monitored by the single-scan method, as a single scan can cover both settlement region and settlement-free region. However, in cases where the monitored position is very close to the tunnelling path, the two-scans registration method is needed. For example, as shown in Figure 15, the settlement marker to be monitored is located close to P5, and the tunneling path is just under P5. In this case, a single scan at P5 cannot capture enough settlement-free region. Therefore, scans are conducted at both P4 and P5, and the two scans are registered as a point cloud dataset to monitor the building settlement near P5. The registration error between these two scans is only 1.2 mm, indicating a good accuracy.

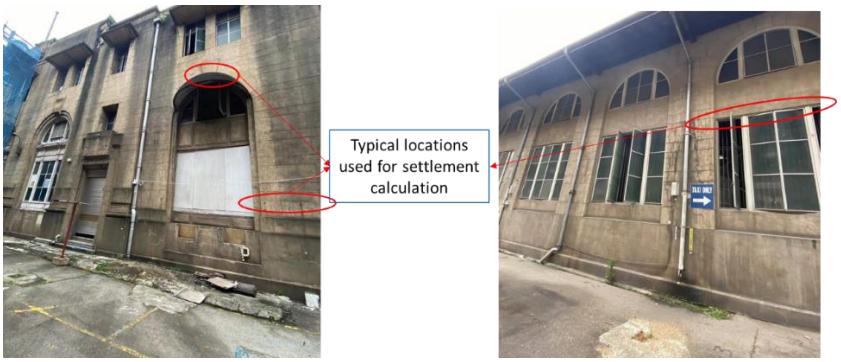

Figure 14. Point selection for building settlement value calculation.

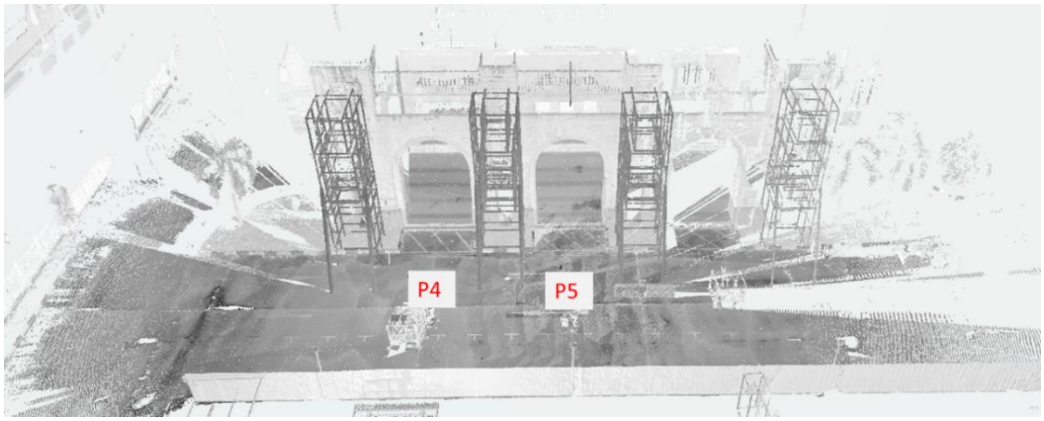

Figure 15. Two-scans registration at A3.

Table 3 and Table 4 show the calculated settlement values at building settlement markers (BM) and ground settlement markers (LG) monitored by LiDAR and the corresponding values measured by traditional survey. It is found that the values obtained through LiDAR data are similar to the values measure by traditional survey. The mean errors for BM series markers and LG series markers are 2.2 mm and 1.8 mm, respectively. The standard deviations are 1.2 mm and 1.6 mm for BM and LG series, respectively. Based on the above results, it could be concluded that the local scan-based method including single scan method and two-scans registration method is generally suitable for monitoring ground and building settlements. In terms of some values with relatively higher errors, such as LG A301 on Day 3 and Day 4, incomplete data for settlement-free region could be the reason that affect the point cloud alignment accuracy. For this specific case, fence of the building is the reason that affects the data completeness, and the solution could be either increasing the scanner height or using two-scans registration method to cover more information for settlement-free region.

Table 3. Settlement values at A3 (BM Series).

	BM A301	**BM A302**	**BM A303**	**BM A305**	**BM A304**	**BM A307**	**BM A306**	**BM A308**	**BM A309**
Day 1	Baseline		-	-	-	-	-	Baseline	-
Day 2	-0.4 (-1.0)	-3.6 (-0.4)			Baseline			-1.9 (-0.3)	Baseline
Day 3	2.9 (-0.5)	1.0 (-0.8)	2.3 (0.9)	2.8 (-0.4)	2.8 (-0.5)	2.2 (-0.6)	2.2 (-0.5)	-1.1 (-0.5)	0.8 (-0.6)
Day 4	2.4 (-1.0)	-2.2 (-0.9)	3.7 (-0.4)	3.7 (-0.9)	3.7 (-1.3)	0.5 (-1.2)	0.5 (-0.9)	-0.7 (-1.1)	1.2 (-0.5)
Day 5	1.4 (-0.1)	-2.8 (-1.6)	1.5 (-1.9)	-0.6 (-1.3)	-0.6 (-1.2)	-4.3 (-1.6)	-4.3 (-1.6)	1.5 (-0.4)	3.4 (0.3)

Table 4. Settlement values at A3 (LG Series).

	LG A301	**LG A302**	**LG A303**	**LG A305**	**LG A304**	**LG A307**	**LG A306**	**LG A308**	**LG A309**
Day 1					Baseline				
Day 2	0.8 (-0.2)	-5.0 (-0.2)	- (0.3)	-1.5 (-0.2)	-1.5 (-0.1)	-1.0 (-0.5)	-1.0 (0.1)	0.1 (0.7)	0.1 (0.3)

Table 4. *Cont.*

	LG A301	LG A302	LG A303	LG A305	LG A304	LG A307	LG A306	LG A308	LG A309
Day 3	4.5 (-0.4)	-1.2 (0.4)	- (-0.5)	0.9 (-0.1)	0.9 (0.0)	0.9 (-0.3)	0.9 (0.2)	-0.1 (0.8)	-0.1 (0.3)
Day 4	5.2 (-1.4)	-0.7 (-0.5)	- (-0.8)	0.8 (-0.6)	0.8 (0.3)	-1.5 (-0.4)	-1.5 (0.8)	3.2 (0.7)	3.2 (-0.2)
Day 5	1.4 (-1.2)	-1.4 (-0.2)	- (-0.4)	-0.3 (-0.7)	-0.3 (0.4)	-4.0 (0.1)	-4.0 (0.4)	1.9 (0.4)	1.9 (-1.7)

4.4. Discussions

Based on the above results, it can be concluded that the local scan-based method has satisfactory accuracy for monitoring the settlement of buildings and ground induced by tunneling. When one single scan cannot cover sufficient settlement-free region information, one more scan can be added. In order to further illustrate the simplicity and accuracy of the method, a comparison between the local scan-based method and the full area registration-based method is conducted.

By adopting the full area registration-based method, more settlement markers in the settlement region can be monitored. However, due to the registration errors, the accuracy of the settlement values obtained can be worse. A comparison is conducted at A2 between local scan-based method and full area registration-based method. Some of the identical ground settlement markers at A2 are used for the comparison. Figure 16 shows the settlement values of some markers at A2 with the full area registration-based method between Day 2 and Day 3. The Z values in the figure are the settlement values, where negative values indicate settlements and positive ones indicate heaves. The settlement values of all the markers in the A2 area can be identified simultaneously by processing the registered point cloud data once.

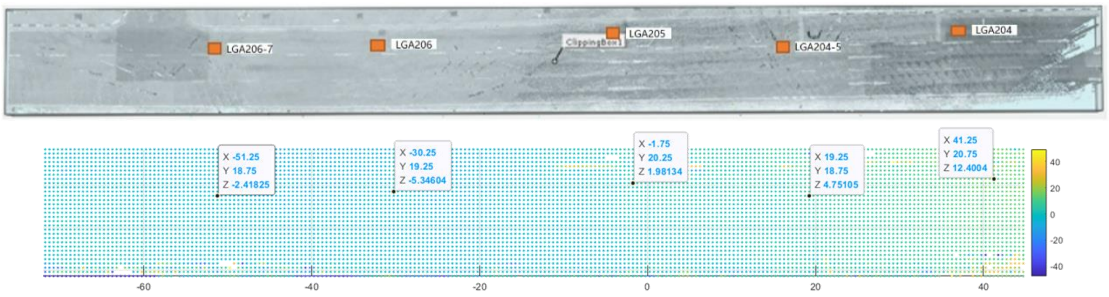

Figure 16. Settlement measurements at A2 based on the full area registration-based method.

Table 5 indicates the settlement measurements for some markers between Day 2 and Day 3 with different methods (traditional survey method, local scan-based method and full area registration-based method). Compared to the traditional survey method, the average errors of the local scan-based method and full area registration-based method are 1.9 mm and 3.8 mm, respectively. Hence, the local scan-based method shows a better accuracy in settlement monitoring.

Table 5. Comparison of settlement values of A2 based on different methods.

	LG A206-7	LG A206	LG A205
Traditional survey method	1.4	2.2	2.0
Local scan-based method	NA	2.1	5.7
Full area registration-based method	-2.4	-5.4	2.0

5. Conclusions and future work

This study presents the monitoring and measurement of ground and building settlements induced by tunneling excavation based on LiDAR technique. A methodology for point cloud processing and settlement measurement including a rough alignment and fine alignment was proposed. The ground settlement along a major road in Singapore was monitored and measured based on LiDAR technique and the proposed method. Different scan strategies including local scan-based method and full area registration-based method were examined and compared with the results obtained from the traditional survey method. Results from the case study showed that LiDAR point cloud data are feasible for monitoring and measuring the ground and building settlements induced by tunnelling excavation at millimeter level, especially for the local scan-based method. Although the full area registration-based method has higher calculation efficiency, its measurement accuracy is not satisfactory.

Some improvements of this study can be made for better engineering application purpose, which are potential topics for future works. (1) Broader application scenarios. This study validated the feasibility of using LiDAR technique on settlement measurement on a major road with viaducts and buildings. Future works may focus on the different ground environments. (2) Automation. The proposed method in the current study still requires some manual works on the point cloud alignment. Future works will focus on the automation of the procedures to achieve fully automated data processing and settlement measurement.

Acknowledgments

This work was funded by the Science and Technology Planning Project of Jiangsu Province of China with grant number BZ2024058.

Conflicts of interests

There is no conflict of interest.

Authors' contribution

Methodology, X.Z.; Data Curation, X.Z., J.L.; Writing-Original Draft, X.Z.; Visualization, J.L.; Formal analysis, J.L.; Supervision, S.C.C. and Q.W.; Project administration, S.C.C.; Writing-Review & Editing, Q.W. and S.C.C.; Conceptualization, Q.W.; Funding acquisition, Q.W.

References

[1] Ye GL, Hashimoto T, Shen SL, Zhu HH, Bai TH. Lessons learnt from unusual ground settlement during Double-O-Tube tunnelling in soft ground. *Tunn. Undergr. Space Technol.* 2015, 49:79–91.

[2] Yiu W, Burd H, Martin C. Finite-element modelling for the assessment of tunnel-induced damage to a masonry building. *Géotechnique* 2017, 67(9):780–794.
[3] Amorosi A, Boldini Dd, De Felice G, Malena M,Sebastianelli M. Tunnelling-induced deformation and damage on historical masonry structures. *Géotechnique* 2014, 64(2):118–130.
[4] Bilotta E, Paolillo A, Russo G,Aversa S. Displacements induced by tunnelling under a historical building. *Tunn. Undergr. Space Technol.* 2017, 61:221–232.
[5] Klar A, Dromy I, Linker R. Monitoring tunneling induced ground displacements using distributed fiber-optic sensing. *Tunn. Undergr. Space Technol.* 2014, 40:141–150.
[6] Zhang L, Ding X, Lu Z. Ground settlement monitoring based on temporarily coherent points between two SAR acquisitions. *ISPRS J. Photogramm. Remote Sens.* 2011, 66(1):146–152.
[7] Roccheggiani M, Piacentini D, Tirincanti E, Perissin D, Menichetti M. Detection and monitoring of tunneling induced ground movements using Sentinel-1 SAR interferometry. *Remote Sens.* 2019, 11(6):639.
[8] Lu S, Ouyang N, Wu B, Wei Y, Tesemma Z. Lake water volume calculation with time series remote-sensing images. Int. J. *Remote Sens.* 2013, 34(22):7962–7973.
[9] Keutterling A, Thomas A. Monitoring glacier elevation and volume changes with digital photogrammetry and GIS at Gepatschferner glacier, Austria. *Int. J. Remote Sens.* 2006, 27(19):4371–4380.
[10] Gonçalves J, Henriques R. UAV photogrammetry for topographic monitoring of coastal areas. ISPRS J. Photogramm. *Remote Sens.* 2015, 104:101–111.
[11] Chen Z, Zhang B, Han Y, Zuo Z, Zhang X. Modeling accumulated volume of landslides using remote sensing and DTM data. *Remote Sens.* 2014, 6(2):1514–1537.
[12] Koch C, Georgieva K, Kasireddy V, Akinci B, Fieguth P. A review on computer vision based defect detection and condition assessment of concrete and asphalt civil infrastructure. A*dv. Eng. Inf.* 2015, 29(2):196–210.
[13] Tang P, Akinci B. Automatic execution of workflows on laser-scanned data for extracting bridge surveying goals. *Adv. Eng. Inf.* 2012, 26(4):889–903.
[14] Wang Q, Kim MK, Cheng JC, Sohn H. Automated quality assessment of precast concrete elements with geometry irregularities using terrestrial laser scanning. *Autom. Constr.* 2016, 68:170–182.
[15] Nahangi M, Haas CT. Automated 3D compliance checking in pipe spool fabrication. *Adv. Eng. Inf.* 2014, 28(4):360–369.
[16] Ordóñez C, Martínez J, Arias P, Armesto J. Measuring building façades with a low-cost close-range photogrammetry system. *Autom. Constr.* 2010, 19(6):742–749.
[17] Su Y, Hashash YM, Liu LY. Integration of construction as-built data via laser scanning with geotechnical monitoring of urban excavation. *J. Constr. Eng. Manage.* 2006, 132(12):1234–1241.
[18] Kashani AG, Crawford PS, Biswas SK, Graettinger AJ, Grau D. Automated tornado damage assessment and wind speed estimation based on terrestrial laser scanning. *J. Comput. Civ. Eng.* 2015, 29(3):04014051.
[19] Kashani AG, Graettinger AJ. Cluster-based roof covering damage detection in ground-based lidar data. *Autom. Constr.* 2015, 58:19–27.
[20] Zhou Z, Gong J, Guo M. Image-based 3D reconstruction for posthurricane residential building damage assessment. *J. Comput. Civ. Eng.* 2016, 30(2):04015015.

[21] González-Aguilera D, Gómez-Lahoz J, Sánchez J. A new approach for structural monitoring of large dams with a three-dimensional laser scanner. *Sensors 2008* 8(9):5866–5883.

[22] Oskouie P, Becerik-Gerber B, Soibelman L. Automated measurement of highway retaining wall displacements using terrestrial laser scanners. *Autom. Constr.* 2016, 65:86–101.

[23] Riveiro B, González-Jorge H, Varela M, Jáuregui DV. Validation of terrestrial laser scanning and photogrammetry techniques for the measurement of vertical underclearance and beam geometry in structural inspection of bridges. *Measurement 2013* 46(1):784–794.

[24] Riveiro B, Jauregui D, Arias P, Armesto J, Jiang R. An innovative method for remote measurement of minimum vertical underclearance in routine bridge inspection. *Autom. Constr.* 2012, 25:34–40.

[25] Teza G, Galgaro A, Zaltron N, Genevois R. Terrestrial laser scanner to detect landslide displacement fields: a new approach. *Int. J. Remote Sens.* 2007, 28(16):3425–3446.

[26] Kurdi FT, Reed P, Gharineiat Z, Awrangjeb M. Efficiency of terrestrial laser scanning in survey works: Assessment, modelling, and monitoring. *Int. J. Environ. Sci. Nat. Res.* 2023, 32(2):556334.

[27] Gharineiat Z, Tarsha Kurdi F, Campbell G. Review of automatic processing of topography and surface feature identification LiDAR data using machine learning techniques. *Remote Sens.* 2022, 14(19):4685.